# Toward anharmonic computations of vibrational spectra for large molecular systems

**ARTICLE** *in* INTERNATIONAL JOURNAL OF QUANTUM CHEMISTRY · MAY 2012

Impact Factor: 1.43 · DOI: 10.1002/qua.23224

# Toward Anharmonic Computations of Vibrational Spectra for Large Molecular Systems

**VINCENZO BARONE,[1] MALGORZATA BICZYSKO,[1,2] JULIEN BLOINO,[1,2] MONIKA BORKOWSKA-PANEK,[3] IVAN CARNIMEO,[1] PAWEL PANEK[3]**

[1]*Scuola Normale Superiore and INSTM M3-Village, piazza dei Cavalieri 7, 56126 Pisa, Italy*
[2]*Dipartimento di Chimica "Paolo Corradini" and INSTM M3-Village Università di Napoli Federico II, Complesso Univ. Monte S. Angelo, via Cintia, 80126 Napoli, Italy*
[3]*Faculty of Chemistry, University of Wroclaw, ul. Joliot-Curie 14, Wroclaw, Poland*

*Received 20 April 2011; accepted 20 June 2011*
*Published online 30 August 2011 in Wiley Online Library (wileyonlinelibrary.com).*
*DOI 10.1002/qua.23224*

**ABSTRACT:** The subtle interplay of several different effects makes the interpretation and analysis of experimental spectra in terms of structural and dynamic characteristics a very challenging task. In this context, theoretical studies can be very helpful, and this is the reason behind the rapid evolution of computational spectroscopy from a highly specialized research field toward a versatile and widespread tool. However, in the case of vibrational spectra of large molecular systems, the most popular approach still relies on a harmonic treatment, because of the difficulty to explore the multidimensional anharmonic potential energy surface. These can be overcome considering that, in many cases, the vibrational transitions are well localized and only some of them are observed experimentally. To this aim, the procedure for the simulation of vibrational spectra of large molecular systems beyond the harmonic approximation is discussed. The quality of system-specific reduced dimensional anharmonic approaches is first validated by comparison with computations taking into account all modes simultaneously for anisole and glycine. Next, the approach is applied to two larger systems, namely glycine adsorbed on a silicon surface and chlorophyll-*a* in solution, and the results are compared with experimental data showing significant improvement over the standard harmonic approximation. Our results show that properly tailored reduced dimension anharmonic approaches stand as feasible routes for state-of-the-art computational spectroscopy studies and allow to take into account both anharmonic and environmental effects on the spectra even for relatively large molecular systems.  Int J Quantum Chem 112: 2185–2200, 2012

**Key words:** spectroscopy; IR; computation; macrosystems

*Correspondence to:* V. Barone; e-mail: vincenzo.barone@sns.it (or) M. Biczysko; e-mail: malgorzata.biczysko@sns.it, J. Bloino; e-mail: julien.bloino@sns.it

Contract grant sponsor: Italian MIUR

## 1. Introduction

Effective in silico solutions of the vibrational problem for polyatomic molecules and simulation of IR and Raman spectra are among the most important tasks of contemporary computational chemistry. Although both time-dependent and time-independent routes have been proposed to this end, in this contribution, we will refer only to time-independent approaches in view of their efficiency and ease of use. Theoretical computations of vibrational frequencies and IR/Raman intensities at the harmonic level have become a routine tool assisting the interpretation of spectroscopic experiments. However, anharmonicity and vibrorotational couplings come into play as soon as accuracy becomes an issue. Ongoing developments to improve software efficiency and enhancements of hardware capabilities enable the calculation of accurate vibrational frequencies for small molecules (up to five to six atoms) by state-of-the-art electronic computations followed by converged variational solutions of the vibrational problem [1, 2]. Extension of the anharmonic treatment to larger systems induces two main scaling problems [3, 4]. The first one concerns the building of the underlying potential energy surface (PES), whereas the second one is related to the solution of the corresponding time-independent Schrödinger equation. Concerning the first point, multilayer methods (such as the ONIOM one [5–8]) can be used to treat only a reduced part of the system, where the studied phenomenon is localized, at a higher level, while taking into account the tuning by the remaining part of the system at a lower level. In several cases, account for environmental (e.g., bulk solvent and low-temperature matrix) effects through continuum models has been advocated and put in use with remarkable results [9, 10]. Additionally, it is possible to use one of the approaches based on the analytical representation of the potential (e.g., expressed in normal or internal coordinates) along with its effective truncation schemes which have been proposed in the last years [11–15]. In our work, we prefer to use normal coordinates expressed in terms of Cartesian coordinates in view of their generality and simplicity of use, especially when dealing with large systems. The PES is then expressed as a polynomial of fourth degree containing at most three independent normal coordinates. Although this scheme presents several known limitations, especially when dealing with large amplitude torsion and inversion motion and/or in presence of double-well potentials, it is well adapted for many phenomena and physical–chemical properties, which are tuned essentially by small amplitude vibrations of a limited number of degrees of freedom around a well-defined energy minimum. In such a situation, a proper selection of the principal degrees of freedom by chemical intuition or using more automatic selection procedures (to be described in the following) must be combined with the effective use of all available information including coupling with other degrees of freedom. Starting from this point, perturbative or variational procedures can be used to solve the vibrational problem. A widely used approach is based on vibrational self-consistent field (VSCF) using a potential truncated to two-, three-, and four-mode couplings [16–23], which is able to describe a large variety of systems, also involving large amplitude motions. Next, correlation is taken into account by vibrational Møller-Plesset perturbation theory (VMP, also known as correlation-corrected VSCF, cc-VSCF) [24, 25], vibrational configuration interaction (VCI) [17, 26], or vibrational coupled clusters (VCC) [27]. The advantages of both perturbative and variational approaches can be integrated by using small VCI matrices dressed by the effect of the other states treated at the VPT2 level [28]. An iterative variational-perturbational scheme has been implemented, for instance, in the VCI-P code [29] and applied to a number of interesting problems. Although such procedures represent, in our opinion, a promising route for the computation of anharmonic frequencies in medium-to-large systems, use of vibrational second-order perturbation theory (VPT2) based on normal modes without any VSCF step [30–43] remains very attractive at least for semirigid systems [44–50]. A particularly effective approach is obtained when the fourth-order representation of the PES is obtained at the DFT level using hybrid (especially B3LYP [51–57]) or double-hybrid (especially B2PLYP [58–61]) functional with medium-size basis sets. Improved results can be obtained by computing the harmonic part of the potential at more advanced levels [52, 57, 62–65]. It is well known that the presence of resonances plagues VPT2 computations of nearly all but the smallest systems. The approach most commonly used in this case is to neglect nearly singular contributions (deperturbed computations). Automatic procedures have been designed to effectively remove interactions in the second-order treatment, which are more properly treated at the first order. For this purpose, several schemes have been introduced (e.g.,

the general criteria proposed by Martin et al. [35]) and such an automated approach has been shown to provide accurate results at least for fundamental bands [48]. More general procedures to solve in an effective way this problem have been also introduced [66]. Additionally, within the VPT2 approach, it is also possible to restrict the anharmonic treatment to a small part of the total system, directly related to the spectroscopic observable of interest, for instance the most intense bands in the IR spectrum, without loosing the benefits of a unified and comprehensive picture. Such a procedure provides a path to extend the anharmonic treatment to complex macromolecular systems, allowing to better describe the subtle features present in experimental vibrational spectra and to gain a deeper insight into several important real-world processes. In the present work, a careful analysis of such reduced-dimensionality VPT2 treatments is provided and the possible recipes to correctly choose normal modes, which need to be included in the anharmonic treatment, without any "a priori" evaluation of all couplings, are proposed and validated.

This article is organized as follows: the practical issues of the reduced-dimensionality perturbative vibrational procedure and theoretical foundations of the proposed treatment are collected in Section 2, whereas computational details are gathered in Section 3. Results for anisole computed with the complete VPT2 model and several reduced-dimensionality schemes are discussed in Section 4.1. The reduced-dimensionality approach is then applied to the studies of two larger systems, namely glycine adsorbed on a silicon surface (4.2) and chlorophyll-*a* in solution (4.3). The results are compared with experimental data and improvements over the standard harmonic computations are discussed. Final remarks about the overall performance of the proposed scheme are collected in Section 5.

## 2. Reduced Dimensionality Vibrational Perturbative Approach

The basis of the fully automated second-order vibrational perturbative implementation has been presented in detail in previous articles [33, 34]. Here, we just recall some details necessary to discuss the reduced dimensionality VPT2 treatment. Let us define the third ($K_{ijk}$) and fourth ($K_{ijkl}$) energy derivatives with respect to the mass-weighted normal coordinates **Q** as:

$$K_{ijk} = \frac{\partial^3 V}{\partial Q_i \partial Q_j \partial Q_k} \quad \text{and} \quad K_{ijkl} = \frac{\partial^4 V}{\partial Q_i \partial Q_j \partial Q_k \partial Q_l}$$

In practice, as described in Ref. 33, all terms with at most three distinct indices, that is to say the third and semidiagonal fourth derivatives, can be evaluated from numerical differentiation of analytical Hessian matrices at geometries displaced by small increments along a single normal coordinate. For a molecular system with $N$ atoms at most 6N-11 Hessian computations are necessary to obtain all terms required to compute the vibrational energy (in wavenumbers) of asymmetric tops within the vibrational perturbative approach, which are given by:

$$E_n = \chi_0 + \sum_i \omega_i \left(n_i + \frac{1}{2}\right) + \sum_i \sum_{j<i} \chi_{ij} \left(n_i + \frac{1}{2}\right)\left(n_j + \frac{1}{2}\right) \quad (1)$$

where the $\omega$'s are the harmonic wavenumbers and the $\chi$'s are the anharmonic contributions given by the following equations [33, 67]

$$64\,h\,c\,\chi_0 = \sum_{i=1}^{N} \frac{K_{iiii}}{\lambda_i} - \frac{7}{9}\sum_{i=1}^{N} \frac{{K_{iii}}^2}{{\lambda_i}^2} + 3\sum_{i=1}^{N}\sum_{\substack{j=1 \\ j\neq i}}^{N} \frac{{K_{ijj}}^2}{\lambda_j(4\lambda_j - \lambda_i)} - 16\sum_{i=1}^{N}\sum_{j=i+1}^{N}\sum_{k=j+1}^{N} \times \frac{K_{ijk}^2}{{\lambda_i}^2 + {\lambda_j}^2 + {\lambda_k}^2 - 2(\lambda_i\lambda_j + \lambda_i\lambda_k + \lambda_j\lambda_k)} - 16\sum_{\alpha=x,y,z} \mu^0_{\alpha\alpha}\left[1 + 2\sum_{i=1}^{N}\sum_{j=i+1}^{N} (\zeta_{ij}^{\alpha})^2\right] \quad (2)$$

$$16\,h\,c\,\lambda_i\,\chi_{ii} = K_{iiii} - \frac{5{K_{iii}}^2}{3\lambda_i} - \sum_{\substack{j=1 \\ j\neq i}}^{N} \frac{(8\lambda_i - 3\lambda_j){K_{iij}}^2}{\lambda_j(4\lambda_i - \lambda_j)} \quad (3)$$

$$4\,h\,c\,\sqrt{\lambda_i\lambda_j}\,\chi_{ij} = K_{iijj} - \frac{2{K_{iij}}^2}{4\lambda_i - \lambda_j} - \frac{2{K_{ijj}}^2}{4\lambda_j - \lambda_i} - \frac{K_{iii}K_{ijj}}{\lambda_i} - \frac{K_{jjj}K_{iij}}{\lambda_j} + \sum_{\substack{k=1 \\ k\neq j,i}}^{N} \times \left[\frac{2(\lambda_i + \lambda_j - \lambda_k){K_{ijk}}^2}{{\lambda_i}^2 + {\lambda_j}^2 + {\lambda_k}^2 - 2(\lambda_i\lambda_j + \lambda_i\lambda_k + \lambda_j\lambda_k)} - \frac{K_{iik}K_{jjk}}{\lambda_k}\right] + 4(\lambda_i + \lambda_j)\sum_{\alpha=x,y,z} \mu^0_{\alpha\alpha}\left(\zeta_{ij}^{\alpha}\right)^2 \quad (4)$$

where $\lambda_i = (2\pi c\omega_i)^2$ and $\zeta_{ij}^{\alpha}$ is the Coriolis coupling constants.

The fundamental bands $\nu_i$, overtones $[2\nu_i]$, and combination bands $[\nu_i + \nu_j]$ are then given by:

$$\nu_i = \omega_i + 2\chi_{ii} + \frac{1}{2}\sum_{\substack{j=1 \\ j\neq i}}^{N} \chi_{ij} \tag{5}$$

$$[2\nu_i] = 2\omega_i + 6\chi_{ii} + \sum_{\substack{j=1 \\ j\neq i}}^{N} \chi_{ij} = 2\nu_i + 2\chi_{ii} \tag{6}$$

$$[\nu_i\nu_j] = \omega_i + \omega_j + 2\chi_{ii} + 2\chi_{jj} + \sum_{\substack{k=1 \\ k\neq j,i}}^{N} (\chi_{ik} + \chi_{ik}) = \nu_i + \nu_j + \chi_{ij} \tag{7}$$

In the following, we will discuss the application of VPT2 to cases where a reduced number of force constants is available for the perturbative treatment. Let us first define a set of $M$ normal modes for which anharmonic frequencies will be evaluated (this corresponds to the SelectAnharmonicModes keyword in Gaussian) that we will refer to as the active modes. Those modes also represent the directions of displacement for the numerical differentiation, so that 2M+1 Hessian needs to be calculated to carry out the perturbative treatment. Then, assuming that index $i$ corresponds to an active mode, all the cubic force constants $K_{ijk}$ where index $i$ is present at least once (i.e., $K_{ijk}$, $K_{ijj}$, $K_{iik}$, $K_{iii}$) will be evaluated along with all $K_{iijj}$ and $K_{iiij}$ quartic force constants. However, in such a reduced-dimensionality treatment a limited number of cubic force constants (terms including only $j$ and $k$ indices) will not be evaluated, and this difference can influence the results in comparison with the full-dimensionality case where all ($K_{ijk}$) and ($K_{iijk}$) are available. Nevertheless, it is noteworthy that in practice there are only two terms in Eq. (4), which might not be computed, namely:

$$\Delta_j = \frac{K_{jjj}K_{iij}}{\lambda_j} \quad \text{and} \quad \Delta_{jk} = \frac{K_{iik}K_{jjk}}{\lambda_k} \tag{8}$$

First of all, it should be stressed that both terms are nonresonant (denominators do not include differences between diverse λ) so that the role of Fermi resonances, if any, remain unchanged. Moreover, these terms, which are only taken into account if both $i$ and $j$ are included in the active set, in most cases should have only little impact on the results. The first term should not be omitted if both $K_{jjj}$ and $K_{iij}$ are large. As $K_{iij}/\lambda_j$ is known, it is possible to have a qualitative estimation of the impact of the whole term in the calculation of $\chi_{ij}$. If it is very small, then it is likely that $\Delta_j$ will give a small contribution and can be safely neglected. A larger value of $K_{iij}$ reflects a significant coupling between modes $i$ and $j$, meaning that mode $j$ must be also included in the set of active modes. Chemical intuition can also help to assess more precisely the magnitude of $K_{jjj}K_{iij}$ by noting that $K_{jjj}$ will be important only if mode $j$ is strongly anharmonic. In such a case, mode $j$ must be included in the set of active modes to be treated anharmonically. If the numerical differentiation along $j$ is too cumbersome and does not have an interest per se (e.g., it is not in the frequency range under study), an alternative approach would be to include only the missing terms $K_{jjj}$ through numerical evaluation of the third derivatives one-dimensional energy, a task much less computationally demanding than the Hessian computations. The second term reflects the coupling of mode $k$ with both modes $i$ and $j$. As before, the known $K_{iik}$ can be used to guess the possible influence of the whole term, which will not contribute to Eq. (4) if $K_{iik}/\lambda_k$ is negligible, that is, if $i$ and $k$ are uncoupled. On the other hand, for large $K_{iik}$ constants, the whole $\Delta_{jk}$ term is not negligible if mode $j$ is also strongly coupled to mode $k$. In practice, if the map of couplings is represented graphically (see for example Figs. 1 and 2 for anisole and glycine, respectively), where the double index $ii$ is represented by the rows and index $k$ by the columns, for each large $K_{iik}$ term it can be checked if there is any normal mode $j$ for which a large coupling with $k$ is also observed. In summary, the reduced-dimensionality approach can be safely applied if all modes, which are strongly coupled are included simultaneously into VPT2 computations, so the necessary force constants are evaluated. The general rules for the definition of reduced-dimensionality normal mode sets, which will be discussed in the following sections, take into account the geometrical confinement of vibrations and the spanned frequency range, because the vibrations localized in different regions of the molecular systems and with significantly different frequencies are unlikely to be strongly coupled. Different schemes to guess a priori coupling strengths based on lower level electronic structure computations, resonance conditions, or normal mode similarity have been proposed (See Ref. 11 and references therein). In the present work, instead, we have chosen to discuss the possibility of couplings from a "chemical"

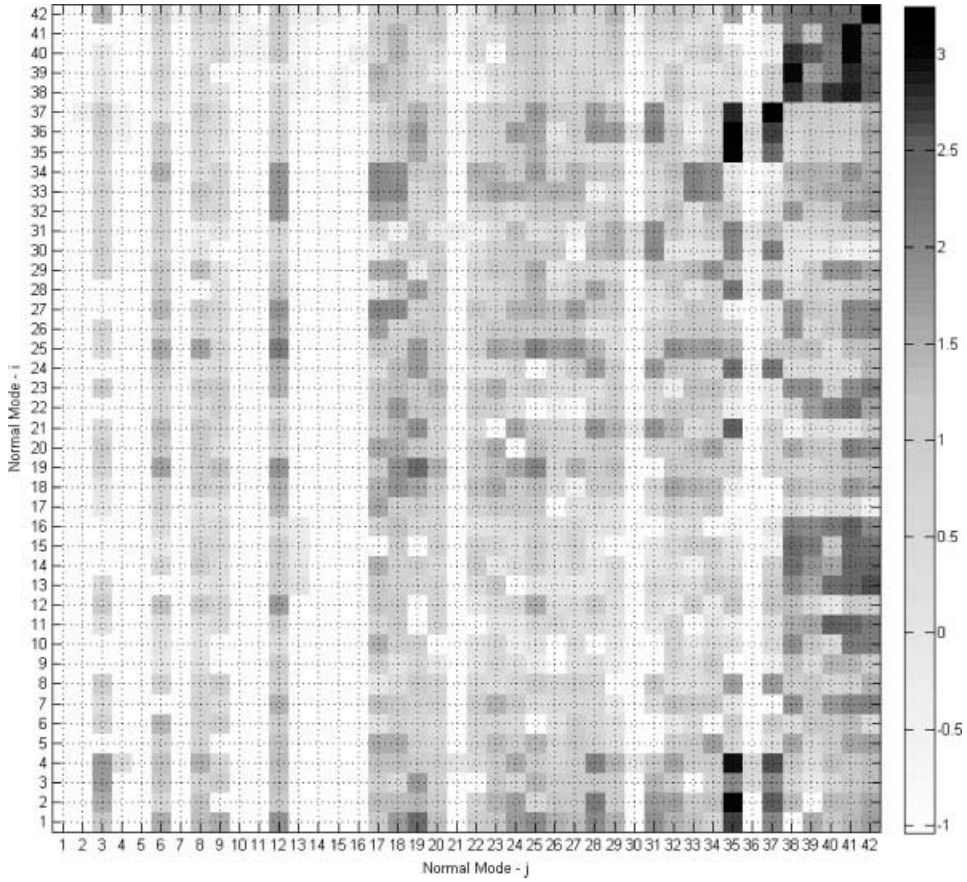


**FIGURE 1.** Graphical representation of the absolute value of the cubic force constants $K_{iij}$ for anisole. A shade of gray is assigned depending on the value of $\log_{10}(|K_{iij}|)$, from white for the values lower than 0.1 to black for values above 3.

point of view, followed by a proper validation of the results.

Concerning macromolecular systems with a large number of normal modes, a proper treatment of Fermi resonances, which are known to plague the VPT2 computations, becomes increasingly important. The most classical approach, which is also implemented in the present work, relies on a procedure to automatically neglect nearly singular contributions (deperturbed computations), effectively removing interactions in the second-order treatment, which are more properly treated at first order. The drawback of such an approach is related to the need of applying arbitrary criteria to define resonances. Although the present implementation, which uses criteria proposed by Martin et al. [35], has been shown to provide accurate results at least for fundamental bands [48], a recently implemented alternative approach represents a significant improvement and should be advocated whenever possible. Here, we just mention that it is possible to solve in a general way the problem of Fermi resonances by modifying Eqs. (2)–(4) so that divergent terms are no longer present [66].

## 3. Computational Details

Density functional theory computations have been performed with the B3LYP/N07D model, using the well-known B3LYP [51] density functional and the recently introduced polarized double-$\zeta$ basis set N07D [68–71] able to provide an optimum compromise between reliability and computer time [56, 57]. In this work, the original N07D basis set constructed by adding a reduced number of polarization and diffuse functions to the 6-31G set (see Refs. 68, 69 for details) has been modified to

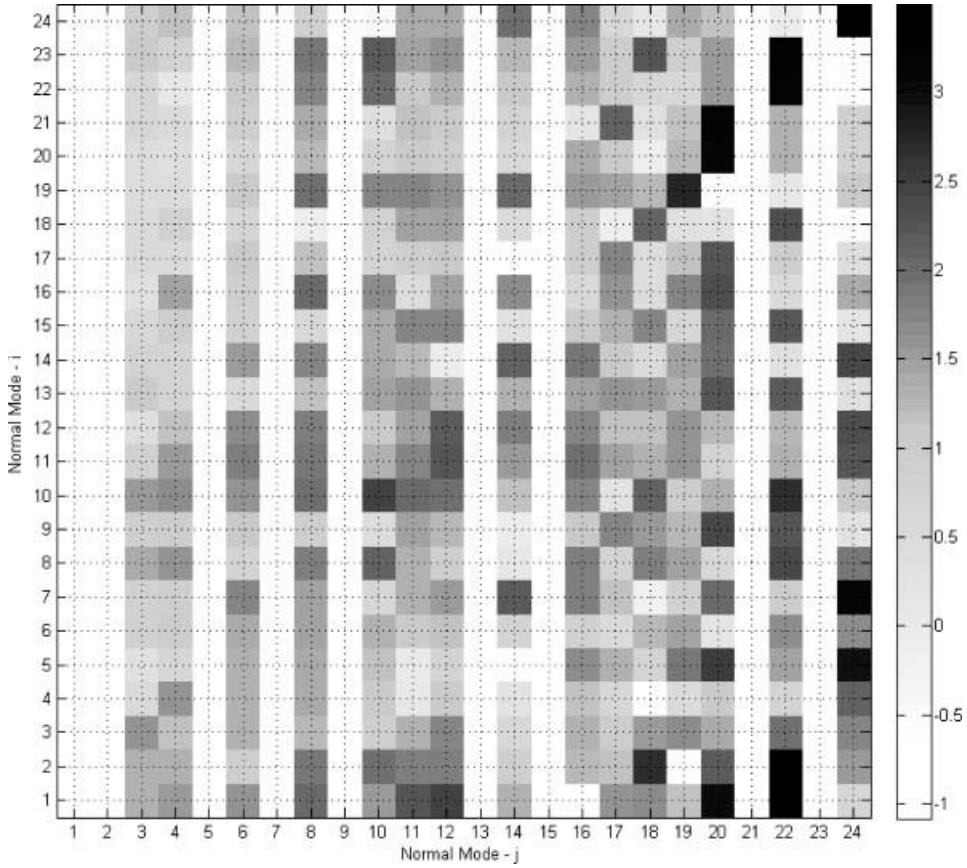


**FIGURE 2.** Graphical representation of the absolute value of the cubic force constants $K_{iij}$ for isolated glycine. A shade of gray is assigned depending on the value of $\log_{10}(|K_{iij}|)$, from white for the values lower than 0.1 to black for values above 3.

include consistently diffuse *s* functions on all heavy atoms as recommended from studies of vinyl radical [56, 72]. This basis set has been further augmented by one set of diffuse *d* functions on heavy atoms leading to the aug-N07D [71] basis set (see supplementary material). All structures have been optimized using tight convergence criteria, and followed by computations of anharmonic frequencies using the second-order perturbative (VPT2) vibrational approach [33]. For the latter, the semidiagonal quartic force field has been evaluated by numerical differentiation (with the standard 0.01-Å step) of analytical second derivatives. Solvent effects on the IR spectrum of chlorophyll *a5* have been simulated by means of a continuum medium within the conductor-like continuum polarizable model (CPCM) [73]. All calculations have been performed with the Gaussian suite of quantum chemistry programs [74].

## 4. Computation of Vibrational Properties with Reduced Dimensionality VPT2 Computations

### 4.1. REDUCED VERSUS FULL DIMENSION COMPUTATIONS OF ANHARMONIC FREQUENCIES FOR ANISOLE

The very good agreement between experimental and theoretical frequencies computed with full-dimensional VPT2 approach has been clearly illustrated recently [50], whereas simulation of anharmonic correction by simple scaling factors led to a comparable overall agreement only if different values were adopted for the high- and low-frequency parts of the spectrum [75]. It is noteworthy that in the latter case, the relative errors affecting a particular frequency are rather arbitrary, whereas for VPT2

computations, small residual discrepancies, when present, are clearly related to the physical nature of the phenomenon [50]. Overall, the anharmonic frequency calculations for anisole listed in Table I represent the most reliable theoretical values and will stand as a reference for the reduced-dimensionality VPT2 computations. To highlight the capabilities of reduced-dimensionality approach, the results from the one-mode VPT2 treatment (referred to as 1M in the following), where each mode has been computed separately are compared with the complete VPT2 treatment where numerical differentiation has been carried out with respect to all normal modes of the system (full-dimensional VPT2 calculation). Table I reports also the data on the most important force constants related to the anharmonic mode-mode couplings, while the absolute values of all $K_{iij}$ are graphically reported in Figure 1 (a darker cell indicates a higher value of $|K_{iij}|$). These results stand as a "pool" of vibrations allowing to analyze impact of various couplings terms on overall results from reduced-dimensionality computations.

It can be observed that for a large number of fundamental frequencies (29 modes out of total 42, marked with an asterisk in Table I), the one-mode approach leads to values similar (within $\approx 15\,cm^{-1}$) to the full-dimensional VPT2 computations. This means that for those normal modes all necessary force constants contain at least one $i$ index, so are evaluated from Hessian computations displaced along single mode of interest. This can be directly related to the fact that these modes do not show strong coupling effects as depicted by the dominance of light tones for most cells of Figure 1 and highlights the good accuracy of 1M computations for normal modes with moderate anharmonic effects. Additionally, the analysis for each row $ii$ of the sum of nondiagonal $|K_{iij}|$ ($\sum_{j\neq i}|K_{iij}|$) and $|K_{iij}|_{max}$, the largest value of $|K_{iij}|$ in the row, allows to assess the accuracy of the reduced-dimensionality VPT2 treatment. In fact, a low value of $|K_{iij}|_{max}$ grants that none of the single couplings with any mode $j$ can lead to significant discrepancies, while the low value of $\sum|K_{iij}|$ assures that the cumulative error due to the omission of small but non-negligible terms has a limited incidence on the overall calculations. The numerical values listed in Table I show that for all modes of anisole for which the 1M approach leads to values close to the full-dimensional (All Modes, AM) VPT2 treatment, $\sum|K_{iij}|$ is smaller than $800\,cm^{-1}$ ($\approx 20\,cm^{-1}$/normal mode), and at the same time none of the $K_{iij}$ constants is larger than $300\,cm^{-1}$ in absolute value. It should be stressed that all the values of $K_{iij}$ are always computed for each mode $i$ included in the set of normal modes $M$ chosen for the anharmonic study, allowing the validation procedure suggested above.

On the other hand, the large discrepancies between the anharmonic frequencies computed with the all-mode and reduced 1-mode models observed for modes 36 ($\nu_{CH_3}$ asym. stretch, $113\,cm^{-1}$) and 37 ($\nu_{CH_3}$ asym. stretch, $33\,cm^{-1}$) can be directly attributed to the significant coupling with mode 35 ($\nu_{CH_3}$ sym. stretch), which is also strongly anharmonic as shown by the large absolute value of $K_{jjj}$ ($-1204\,cm^{-1}$). In fact, as shown in Table II, when such a coupling is considered and modes 36 and/or 37 are computed simultaneously with mode 35, the agreement with full-dimensional VPT2 computations for these modes is very good. It shall be noted that modes 35–37 are all related to the symmetric and asymmetric stretching vibration of the $CH_3$ group, so that the possibility of important coupling effects, which should not be neglected can be also deduced from chemical observation. It can be also noted that inclusion of couplings with antisymmetric $\nu_{CH_3}$ stretching modes do not modify the results for the symmetric $\nu_{CH_3}$ stretching mode with respect to the 1M case. Such a result can be attributed to the fact that mode 35 is coupled to several other modes (see the column related to the $j_{max}$ index in Table I), leading to a diminished effectiveness of the reduced-dimensionality approach. Nevertheless, it is noteworthy that in this case, the reduced VPT2 treatment ($2897\,cm^{-1}$) leads to a significant improvement over the harmonic value of $3009\,cm^{-1}$, and also over the simplest one-dimensional model where PES is expanded along one mode only, completely neglecting all coupling terms. In the latter case the one-dimensional quartic PES is describe through the terms $K_{ii}$, $K_{iii}$, and $K_{iiii}$ leading to the frequency of $2962\,cm^{-1}$.

Analysis of Figure 1 shows also significant couplings between all modes related to the aromatic ring C–H stretching vibrations, where rather large deviations between one-mode and all-mode approaches are observed. In Table II, this group of modes is analyzed together with the $\nu_{10a}$ ring deformation (mode 13), which is coupled to the higher frequency mode $\nu_2$. First, all modes 38–42 are computed together (5M approximation) leading for each mode to a significant improvement over the 1M reduced-dimensionality approximation, with discrepancies with respect to the full-dimensional treatment lower than $15\,cm^{-1}$. Mode 4 reduced-dimensionality treatment includes the modes $\nu_{10a}$ and 40, 41, and 42

**TABLE I**

**Anharmonic vibrational frequencies of anisole, computed with complete VPT2 treatment (All-Modes - AM) and considering mode one-by-one (1-mode - 1M).**

| Mode[a] | Assignment[b] | Exp[c] | AM | SE | 1M | SE | ΔAM | $\sum \lvert K_{iij} \rvert$ | $\lvert K_{iij} \rvert_{max}$ | $j_{max}$ |
|---|---|---|---|---|---|---|---|---|---|---|
| 1 | $\nu_{COC}$ torsion | 82 | 80 | −2 | 59 | −23 | −21 | 1696 | 481 | 35 |
| 2 | $\nu_{10b}$ | 209 | 188 | −21 | 177 | −32 | −11 | 2138 | 1153 | 35 |
| 3* | $\nu_{COC}$ bending | 260 | 248 | −12 | 261 | 1 | 13 | 473 | 85 | 35 |
| 4 | $\nu_O$–$CH_3$ torsion | 263 | 247 | −16 | 273 | 10 | 26 | 1798 | 861 | 35 |
| 5* | $\nu_{16a}$ | 415 | 413 | −2 | 407 | −8 | −7 | 410 | −48 | 34 |
| 6* | $\nu_{9b}$ | 430 | 439 | 9 | 441 | 11 | 2 | 144 | −21 | 41 |
| 7* | $\nu_{16b}$ | 511 | 504 | −7 | 494 | −17 | −10 | 551 | 111 | 42 |
| 8* | $\nu_{6a}$ | 553 | 554 | 1 | 558 | 5 | 4 | 270 | 52 | 37 |
| 9* | $\nu_{6b}$ | 618 | 618 | 0 | 618 | 0 | 1 | 137 | −27 | 41 |
| 10* | $\nu_4$ | 690 | 679 | −11 | 675 | −15 | −4 | 433 | 142 | 42 |
| 11 | $\nu_{11}$ | 752 | 747 | −5 | 729 | −23 | −18 | 813 | −283 | 40 |
| 12* | $\nu_1$ | 788 | 785 | −3 | 787 | −1 | 3 | 225 | −37 | 25 |
| 13 | $\nu_{10a}$ | 819 | 811 | −8 | 788 | −31 | −23 | 1056 | 417 | 42 |
| 14 | $\nu_{17b}$ | 880 | 876 | −4 | 859 | −21 | −17 | 922 | −270 | 41 |
| 15 | $\nu_{17a}$ | 956 | 950 | −6 | 933 | −23 | −17 | 876 | 237 | 38 |
| 16 | $\nu_5$ | 975 | 960 | −15 | 943 | −32 | −17 | 815 | −322 | 41 |
| 17* | $\nu_{12}$ | 997 | 993 | −4 | 998 | 1 | 4 | 152 | 23 | 12 |
| 18* | $\nu_{18a}$ | 1022 | 1024 | 2 | 1028 | 6 | 4 | 471 | −52 | 41 |
| 19* | $\nu_O$–$CH_3$ stretch. | 1039 | 1045 | 6 | 1047 | 8 | 2 | 597 | 104 | 25 |
| 20* | $\nu_{18b}$ | 1073 | 1081 | 8 | 1086 | 13 | 5 | 554 | −111 | 41 |
| 21* | $\nu_{CH_3}$ rock. | 1143 | 1145 | 2 | 1153 | 10 | 9 | 730 | 298 | 35 |
| 22* | $\nu_{15}$ | 1151 | 1161 | 10 | 1157 | 6 | −5 | 578 | −200 | 41 |
| 23* | $\nu_{9a}$ | 1169 | 1176 | 7 | 1177 | 8 | 1 | 595 | 144 | 42 |
| 24* | $\nu_{CH_3}$ rock. | 1180 | 1177 | −3 | 1193 | 13 | 16 | 692 | 177 | 35 |
| 25* | $\nu_{7b}$ | 1253 | 1245 | −8 | 1257 | 4 | 12 | 841 | 130 | 12 |
| 26* | $\nu_3$ | 1292 | 1312 | 20 | 1316 | 24 | 4 | 500 | 84 | 42 |
| 27* | $\nu_{14}$ | 1332 | 1341 | 9 | 1351 | 19 | 10 | 708 | 95 | 17 |
| 28* | $\nu_{CH_3}$ sym. def. | 1442 | 1462 | 20 | 1473 | 31 | 11 | 449 | 158 | 35 |
| 29* | $\nu_{19b}$ | 1455 | 1454 | −1 | 1459 | 4 | 6 | 537 | −74 | 41 |
| 30* | $\nu_{CH_3}$ antisym. def. | 1452 | 1462 | 10 | 1476 | 24 | 14 | 424 | 121 | 37 |
| 31* | $\nu_{CH_3}$ antisym. def. | 1464 | 1460 | −4 | 1469 | 5 | 9 | 286 | 105 | 35 |
| 32* | $\nu_{19a}$ | 1497 | 1498 | 1 | 1505 | 8 | 7 | 478 | 62 | 42 |
| 33* | $\nu_{8b}$ | 1588 | 1589 | 1 | 1605 | 17 | 16 | 714 | 94 | 17 |
| 34* | $\nu_{8a}$ | 1599 | 1606 | 7 | 1618 | 19 | 12 | 779 | −115 | 33 |
| 35 | $\nu_{CH_3}$ sym. stretch. | 2900 | 2856 | −44 | 2897 | −3 | 41 | 460 | 230 | 37 |
| 36 | $\nu_{CH_3}$ asym. stretch. | 2942 | 2930 | −12 | 2817 | −125 | −113 | 2341 | −1347 | 35 |
| 37 | $\nu_{CH_3}$ asym. stretch. | 3004 | 2997 | −7 | 2964 | −40 | −33 | 1041 | −626 | 35 |
| 38 | $\nu_{13}$ | 3026 | 3053 | 27 | 3030 | 4 | −23 | 1824 | 712 | 41 |
| 39 | $\nu_{7a}$ | 3037 | 3046 | 9 | 3017 | −20 | −28 | 2249 | −996 | 38 |
| 40 | $\nu_{20a}$ | 3062 | 3063 | 1 | 3026 | −36 | −37 | 2265 | 1056 | 41 |
| 41* | $\nu_{20b}$ | 3092 | 3071 | −21 | 3063 | −29 | −8 | 660 | −197 | 40 |
| 42 | $\nu_2$ | 3105 | 3083 | −22 | 3072 | −33 | −10 | 1111 | −224 | 41 |
| | | | MUE | 9 | | 18 | 15 | | | |

Signed Error (SE) and mean unsigned error (MUE) with respect to experimental results are reported along with the difference between anharmonic frequencies computed through 1-Mode and All-Modes approach (ΔAM). Sum of non-diagonal cubic force constants, $\sum \lvert K_{iij} \rvert$ with respect to $i$th normal mode and the value of the largest anharmonic contribution to the $i$th normal mode $\lvert K_{iij} \rvert_{max}$, and the corresponding $j_{max}$ index are also reported.

[a]Modes for which anharmonic couplings can be safely neglected are marked by an asterisk.

[b]Assignment from the Ref. [50].

[c] Experimental results from the Ref. [76].

**TABLE II**

**Differences between anharmonic vibrational frequencies computed with limited dimensionality VPT2 treatments and All-Modes approach (ΔAM) for selected normal modes of anisole.**

| Mode | Assignment[a] | Exp[b] | AM | 1M | ΔAM | 5M | ΔAM | 4M | ΔAM | 6M | ΔAM |
|---|---|---|---|---|---|---|---|---|---|---|---|
| | Ring vibrations | | | | | | | | | | |
| 13 | $\nu_{10a}$ | 819 | 811 | 788 | −23 | | | 809 | −2 | 811 | 0 |
| 38 | $\nu_{13}$ | 3026 | 3053 | 3030 | −23 | 3038 | −15 | | | 3043 | −10 |
| 39 | $\nu_{7a}$ | 3037 | 3046 | 3017 | −28 | 3045 | −1 | | | 3053 | 7 |
| 40 | $\nu_{20a}$ | 3062 | 3063 | 3026 | −37 | 3058 | −5 | 3032 | −31 | 3067 | 4 |
| 41 | $\nu_{20b}$ | 3092 | 3071 | 3063 | −8 | 3066 | −6 | 3059 | −13 | 3074 | 3 |
| 42 | $\nu_2$ | 3105 | 3083 | 3072 | −10 | 3089 | 6 | 3082 | −1 | 3089 | 6 |
| | | MUE | 16 | 24 | | 13 | | 20 | | 13 | |
| | $CH_3$ | | | | | | | | | | |
| 35 | $\nu_{CH_3}$ sym. stretch. | 2900 | 2856 | 2897 | 41 | 2898 | 42 | 2892 | 36 | 2898 | 42 |
| 36 | $\nu_{CH_3}$ asym. stretch. | 2942 | 2930 | 2817 | −113 | 2924 | −6 | 2913 | −16 | | |
| 37 | $\nu_{CH_3}$ asym. stretch. | 3004 | 2997 | 2964 | −33 | 2992 | −5 | | | 2992 | −5 |
| | | MUE | 21 | 56 | | 11 | | 18 | | 7 | |

Results from 1-Mode (1M) approximations or including only the most important couplings with other modes (Set n) are reported.

[a]Assignment from the Ref. [50].

[b]Experimental results from the Ref. [76].

computed together, so as to include the most significant couplings starting from mode $\nu_{10a}$ ($j_{max}$ values of 42, 41, 40, and 41 for modes 13, 42, 41, and 40, respectively). Such an approach leads for modes 13 and 42 to results within 2 $cm^{-1}$ from AM computations but does not improve significantly frequencies of modes 40 and 41. The latter are also strongly coupled with other aromatic ring C−H stretching vibrations, as confirmed by the good accuracy obtained for 6M approach, for which modes 38 to 42 have been computed together with mode 13.

In summary, the analysis of vibrational frequencies and couplings for anisole shows that for a large number of normal modes all necessary coupling terms can be evaluated by computing force constants from the numerical differentiation of analytical Hessians along the mode of interest. In such cases, each reduced-dimensionality model considering modes of interest only (even only one mode) leads to results comparable to the VPT2 computations with the full-dimensional treatment. On the other hand, if anharmonic couplings are significant, groups of modes of interest can be computed together in order to take into account otherwise neglected terms. The validation of the reduced-dimensionality approximation can be supported by the analysis of the $K_{iij}$ coupling terms, while the choice of modes, which are strongly coupled and shall be computed together, can be identified by considering the normal mode localization and frequency ranges (here, symmetric and asymmetric stretching vibrations of the $CH_3$ group, C−H ring vibrations).

### 4.2. VIBRATIONAL PROPERTIES OF ISOLATED GLYCINE AND GLYCINE ADSORBED ON SI(100) SURFACE

In this section, we will discuss the computation of anharmonic frequencies of glycine molecule isolated and adsorbed on a Si(100) surface, modeled by a $Si_{15}H_{16}$ cluster. For the former, several studies of the infrared spectrum have shown [77–79] that both perturbative [33] and variational [20] approaches lead to a very good agreement between available experimental data and computed anharmonic vibrational frequencies. It has also been suggested that in the case of glycine, MP2 force fields in conjunction with basis sets of at least augmented double-$\zeta$ quality are required for anharmonic computations. However, we have recently shown [80] that a very good accuracy could be achieved with DFT using the B3LYP [51] functional and the aug-N07D [68–71] basis set, with a mean unsigned error lower than 11 $cm^{-1}$, in line with previous observations made for several other molecules [56, 57, 60]. Consequently, the latter combination of functional and basis set has been chosen in the present study. It can be also noted that the VPT2 computations at the B3LYP/aug-N07D level lead to a better agreement with experiment

than the application of system-optimized scaling factors on harmonic frequencies, which present MUE of 16 and 18 $cm^{-1}$ with maximum absolute discrepancies of 47 and 72 $cm^{-1}$ depending on whether the factors are optimized for the high-frequency region (0.956) or the whole energy range (0.972), respectively. Prior to proceed with the reduced dimensionality VPT2 anharmonic computations for the glycine adsorbed on the $Si_{15}H_{16}$ cluster, an extensive analysis of the couplings between the normal modes of isolated glycine has been performed. To this aim, all couplings have been evaluated through full-dimensional VPT2 computations and the resulting cubic force constants $K_{iij}$ and diagonal matrix elements $K_{iii}$ are reported schematically in Figure 2. In particular, we will focus our discussion on the five normal modes with the highest frequencies, for which discrepancies larger than 100 $cm^{-1}$ between calculated harmonic and experimental frequencies [81–83] (see Table III) indicate large anharmonic effects.

Analysis of the anharmonic terms $K_{iij}$ and $K_{iii}$ allows to associate these large anharmonicities to different contributions. For mode 24, corresponding to the OH stretching frequency, the anharmonic effects are mainly due to the intrinsic anharmonicity of the associated one-dimensional PES. This is indicated by the large $K_{iii}$ force constant for this mode, and significantly lower $K_{iij}$ terms related to the couplings with other modes $j$. In fact, the largest $K_{iij}$ term (96 $cm^{-1}$) is related to the coupling with mode 14, which show a relatively low $K_{iii}$ (122 $cm^{-1}$). A negligible influence of coupling terms is confirmed by 1M (1-mode) VPT2 computation for mode $\nu_{OH}$, which leads to a frequency only 7 $cm^{-1}$ lower than the one obtained when considering all modes at the anharmonic level, and the inclusion of mode 14 improves results by only 3 $cm^{-1}$. Consequently, in the case of mode 24, couplings not included in 1M treatment can be safely neglected and such approximation is sufficient to compute accurately the OH stretching frequency of glycine. Analogous considerations can be made for mode 20, for which the 1M calculations give a frequency of 2916 $cm^{-1}$, in good agreement with the corresponding value of 2938 $cm^{-1}$ obtained from all mode computations.

On the other hand, the anharmonic character of modes 21 and 23 (respectively, $\nu_{CH_2 as}$ and $\nu_{NH_2 as}$) is largely due to the cubic force constants $K_{iij}$. For mode 23, significant interactions with modes 8, 10, 18, and 22 have been found, with the most important coupling involving mode 22 ($\nu_{NH_2 s}$). In fact, inclusion of such a coupling leads to a frequency

**TABLE III.** Differences between anharmonic vibrational frequencies computed with reduced-dimensionality VPT2 treatments and All-Modes approach (ΔAM) for selected normal modes of glycine.

| Label | Assignment | Exp.[a] | AM | SE | 1M | SE | ΔAM | 5M | SE | ΔAM | 6M[b] | SE | ΔAM | $K_{iii}$ | $\sum \lvert K_{iij} \rvert$ | $\lvert K_{iij} \rvert_{max}$ | $j_{max}$ |
|---|---|---|---|---|---|---|---|---|---|---|---|---|---|---|---|---|---|
| 24 | $\nu$(OH) | 3585[c] | 3568 | −17 | 3561 | −24 | −7 | 3561 | −24 | −7 | 3561 | −24 | −7 | 2570 | 289 | 96 | 14 |
| 23 | $\nu(NH_2)a$ | 3410[d] | 3407 | −3 | 3048 | −362 | −359 | 3393 | −17 | −14 | 3411 | 1 | 4 | – | 2255 | 1645 | 22 |
| 22 | $\nu(NH_2)s$ | 3357[e] | 3387 | 30 | 3345 | −12 | −42 | 3342 | −15 | −45 | 3354 | −3 | −33 | 1617 | 302 | 114 | 10 |
| 21 | $\nu(CH_2)a$ | – | 2929 | | 2859 | | −70 | 2931 | | 2 | 2930 | | 1 | 1647 | 1405 | 20 | |
| 20 | $\nu(CH_2)s$ | 2939[e] | 2938 | −1 | 2916 | −23 | −22 | 2913 | −26 | −25 | 2913 | −26 | −25 | 1345 | 134 | 25 | 16 |
| | | MUE | | 10 | | 84 | | | 16 | | | 11 | | | | | |

Results from 1-Mode (1M) approximations or including only the most important couplings with other modes (nM) are reported.
[a]Experimental data from molecular beam and low-temperature matrix environment, the most reliable data for each frequency has been reported, in line what discussed in Carnimeo et al. (submitted for publication).
[b]Coupling with mode 10 included.
[c]Experimental results from Ref. [81].
[d]Experimental results from Ref. [82].
[e]Experimental results from Ref. [83].

of 3392 $cm^{-1}$, in good agreement with the value of 3407 $cm^{-1}$ obtained through a full-dimensional VPT2 treatment, which represents an improvement of more than 50 $cm^{-1}$ with respect to the value from 1M VPT2 computations (3038 $cm^{-1}$). Further refinement of the frequency of mode 23 is achieved with the additional inclusion of mode 10, which leads to an agreement within 5 $cm^{-1}$ with respect to AM computations (3410 $cm^{-1}$), while the subsequent inclusion of contributions from modes 8 and 18 has a negligible effect, leading to frequency values of 3407 and 3405 $cm^{-1}$, respectively. So, to a first approximation, a good overall accuracy for mode $\nu_{NH_2as}$ is obtained including only the coupling with the symmetric stretching mode $\nu_{NH_2}$, while contributions from mode 10 can be included for a further small improvements of the frequency. The same observations can be made for mode 21 ($\nu_{CH_2as}$), which is coupled to modes 17 and 20 ($\nu_{CH_2s}$). In this case, a frequency of 2859 $cm^{-1}$ is obtained from 1M calculation, to be compared with the value of 2929 $cm^{-1}$ when all modes are considered. Reduced-dimensionality 2M calculations, where both $NH_2$ stretching modes are included lead to a frequency of 2933 $cm^{-1}$ for mode 21, in close agreement with the full-dimensional treatment, while VPT2 computations with three active modes, including also mode 17, do not improve further results. Thus, only mode 20 shows relevant contributions to the frequency of mode 21.

For the remaining high frequency mode 22 ($\nu_{NH_2s}$), both large intrinsic anharmonicity of the PES and significant coupling effects contribute to the overall anharmonicity. Indeed, 1M calculations give value of 3345 $cm^{-1}$, to be compared with 3387 $cm^{-1}$ from the full-dimensional VPT2 treatment, and 3506 $cm^{-1}$ from harmonic computations. The further inclusion of the coupling with mode 10 leads to a frequency higher by 10 $cm^{-1}$ while addition of the coupling with mode 8 do not show further improvements.

The above results are consistent with the analysis of different anharmonic terms performed in Sections 2 and 4.1 confirming that for all modes, which do not show large $\Delta_j$, the 1M approach leads to quantitatively accurate results. Otherwise, when large specific couplings are observed, their influence on the overall frequency is enhanced when the intrinsic anharmonicity of each coupled mode is significant. For the high-frequency modes discussed above, the couplings with modes 8, 14, 17, and 18 (which show low intrinsic anharmonicities as described by $K_{jjj}$ of 66, 122, 53, and 124 $cm^{-1}$, respectively) can be safely neglected. On the other hand, couplings with modes 20 and 22 (with $K_{jjj}$ of 1345 and 1617 $cm^{-1}$, respectively) need to be included in the reduced dimensionality VPT2 calculations, while smaller contributions are provided by the inclusion of mode 10 ($K_{jjj}$ of 293 $cm^{-1}$), which can be relevant only when frequencies of modes 22 and 23 have to be computed with high accuracy.

Based on the detailed analysis described above, it is possible to identify the set of normal modes, which need to be considered simultaneously to compute the anharmonic frequencies of the five high-energy modes with an accuracy comparable to the full-dimensional VPT2 treatment. The pertinent anharmonic couplings indicate that modes $\nu_{CH_2s}$ and $\nu_{OH}$ can be computed independently from any other mode (1M approach), while the inclusion of coupling terms is necessary for the accurate computations of stretching mode $\nu_{CH_2as}$ and both symmetric and asymmetric $\nu_{NH_2}$ stretching ones. Thus, in line with the covered energy range, VPT2 computations considering all five highest frequency modes are sufficient to achieve reliable results in this spectral region of isolated glycine molecule.

The same computational model has been applied to the vibrational study of a hybrid system, glycine adsorbed on a silicon cluster, simulating Si(100) surface. Such a computational scheme allows for the direct comparison of computed frequencies and vibrational properties on adsorption on the Si(100) surface. The total system, composed of the glycine molecule and a $Si_{15}H_{16}$ cluster has 117 normal modes, thus the full-dimensional VPT2 anharmonic treatment would require 235 Hessian computations. While such computations would be feasible, especially applying the QM/MM scheme, they can still remain cumbersome. In fact, the only anharmonic computations performed till now for glycine@Si(100), applying the VSCF methodology, was based on the description of the whole system at semiempirical level [84].

At variance, a reduced-dimensionality VPT2 approach allows to combine both the accuracy of the anharmonic treatment and the feasibility of calculations, permitting an accurate QM treatment of the associated anharmonic PES. For the complex system of Glycine@Si(100), the partial VPT2 treatment of the five highest frequency modes has been compared with the computations where all normal modes of adsorbed molecule have been included in the anharmonic treatment (Carnimeo et al., submitted for publication). It shall be noted that the latter approach is feasible even if the whole "molecule+cluster" system is described at the DFT level, due to significant

**TABLE IV**

**Vibrational properties of glycine adsorbed on the $Si_{15}$ cluster.**

| Label | Assignment | Exp.[a] | harm | scaled[b] | SE | 5M | SE | GlyM | SE | ΔAM Gly | $K_{iii}$ | $\sum \lvert K_{ij} \rvert$ | $\lvert K_{ij} \rvert_{max}$ | $j_{max}$ |
|---|---|---|---|---|---|---|---|---|---|---|---|---|---|---|
| 117 | $\nu(NH_2)a$ | 3460 | 3592 | 3434 | −26 | 3405 | −55 | 3419 | −41 | 14 | 181 | 2392 | 1643 | 116 |
| 116 | $\nu(NH_2)s$ | 3410 | 3514 | 3359 | −51 | 3354 | −56 | 3379 | −31 | 25 | 1623 | 470 | 101 | 80 |
| 115 | $\nu(CH_2)a$ | 3040 | 3093 | 2957 | −83 | 2945 | −95 | 2932 | −108 | 13 | 1422 | 1381 | 934 | 114 |
| 114 | $\nu(CH_2)s$ | 2940 | 3041 | 2907 | −33 | 2903 | −37 | 2901 | −39 | 2 | 1620 | 774 | 398 | 115 |
| 112 | $\nu$(SiH) | 2115 | 2186 | 2090 | −25 | 2112 | 3 | 2110 | −5 | 2 | 1124 | 894 | 142 | 107 |
| | | MUE | 92 | 44 | 49 | | 45 | | | | | | | |

Differences between anharmonic vibrational frequencies computed with reduced-dimensionality VPT2 treatments including high-frequency only (5M) or all normal modes of glycine are reported along with values estimated by scaling of harmonic frequencies.

[a]Experimental data from HREEL (high-resolution electron energy loss) spectrum. [85].

[b]System-optimized scaling factor (0.956) obtained for high-frequency normal modes of isolated glycine.

reduction of dimensionality with respect to the AM computations.

The five highest frequency modes of adsorbed glycine are reported in Table IV and compared with experimental results from high resolution electron energy loss (HREEL) spectra [85]. It should be noted that the OH stretching is not present in the adsorbed molecule due to the dissociative character of the adsorption process (see reference Carnimeo et al. submitted for publication, and references therein), while the Si–H stretching, representative of the new system, is reported. Furthermore, a close similarity of $CH_2$ and $NH_2$ stretching modes has been found between isolated and adsorbed glycine.

For adsorbed glycine, in analogy to isolated molecule, $\nu_{NH_2}$ asymmetric stretching is characterized by a low intrinsic anharmonicity and strong coupling effects, which are mainly due to the coupling with mode 116 ($\nu_{NH_2 s}$). In fact, beside this $K_{iij}$ of 1643 $cm^{-1}$ reported in Table IV, all the other coupling constants show values lower than 180 $cm^{-1}$. In variance, for mode 115, an enhanced intrinsic anharmonicity has been observed, along with couplings similar to the ones observed for isolated glycine molecule, which are mainly due to the interaction with $CH_2$ symmetric stretching mode.

Regarding modes 114 and 116, related to symmetric stretch of $\nu_{CH_2}$ and $\nu_{NH_2}$, respectively, large intrinsic anharmonicity effects in conjunction with moderate couplings are observed. The latter ones are particularly relevant for mode 114, for which the overall coupling effect ($\sum |K_{iij}|$ of 774 $cm^{-1}$) is largely due to the cubic constant of 398 $cm^{-1}$ associated to the interaction with $\nu_{CH_2}$ asymmetric stretching mode. It can be also noted that the mode 80 involved in the coupling with the $\nu_{NH_2}$ symmetric stretch is analogous to the mode 10 in isolated glycine. So, it can be concluded that both isolated and adsorbed glycines show similar pattern of anharmonic effects.

From the modes reported in Table IV the stretching Si−H is the only one coupled with modes issuing from $Si_{15}H_{16}$ cluster vibrations, but as indicated by analysis of $K_{iij}$ ($|K_{iij}|_{max} = 142\ cm^{-1}$) and good agreement with experimentally observed frequency, such couplings can be safely neglected. More in general, among all other modes of glycine, the largest coupling with cluster modes ($|K_{iij}|_{max} = 122\ cm^{-1}$), have been found for mode 59 with anharmonic frequency of 567 $cm^{-1}$, which is delocalized over the whole system.

These considerations allow to state confidently that AM Gly computations include all the relevant terms contributing to vibrational frequencies of adsorbed glycine. The frequencies reported in Table IV show that the five-mode model agrees well with frequencies computed including all modes of glycine (a maximum discrepancy of 25 $cm^{-1}$ for mode 116), so that all the most important couplings have been included in the set of the five active modes. Thus, in case if only high-frequency vibrations are of interest a 5M reduced-dimensionality approach is sufficient for reliable comparison with experimental data.

From a comparison between theoretical and experimental frequencies shown in Table IV, a global good agreement is found for all modes but 115. The large discrepancy on the latter is mainly due to an ambiguous assignment of experimental frequency, as suggested and discussed in detail in Carnimeo et al. (submitted for publication). Table IV reports also frequencies obtained from harmonic values scaled by system-specific factor optimized for high-frequency normal modes of isolated glycine. Such ad hoc approach leads to results of overall accuracy similar to discussed reduced-dimensionality

anharmonic models, but with decreased accuracy (error larger by 20 $cm^{-1}$) for $\nu_{SiH}$, the normal mode not present in isolated molecule.

Results presented for glycine and Gly@Si(100) show that the same computational strategy and electronic structure model can be applied to the studies of isolated molecule and complex system involving interaction with the surface or nanoparticle, leading in both cases to good agreement with experimental data and allowing detailed analysis of environmental effects (Carnimeo et al., submitted for publication).

### 4.3. VIBRATIONAL PROPERTIES OF CHLOROPHYLL-*A* IN SOLUTION

The general structural properties of photosystem (PS) II and the sequence of events involved in the light harvesting have already been established [86–89]. However, the underlying detailed molecular mechanism tuning the chemical and photochemical reactivities of PSs is still largely unexplored. Several aspects on the molecular factors enabling a photosynthetic unit to function efficiently, as for example, the supramolecular organization of the system can be effectively studied by spectroscopic techniques. In this respect, the IR spectral region can be extremely informative, as changes in bond strength for C=O, C=C, O−H, N−H, and the breaking or formation of bonds give rise to very specific signatures.

In this respect, the accurate analysis of vibrational spectra of chlorophyll-*a* monomer stands as a base to interpret spectra of more complex systems. Thus, its unequivocal assignment and understanding are of great importance. In practice, assignment of bands in "cation-neutral" difference spectra of chlorophyll-*a* were first made nearly 20 years ago, and since then stand as the basis for the analysis of other "cation minus neutral" FTIR difference spectra obtained for all photosynthetic systems. Some questions on these assignments have been recently raised, based on the comparison with vibrational spectra computed at harmonic level, in the gas phase and solution [90, 91]. Inclusion of anharmonic effects can further improve agreement with observed experimental data, allowing better understanding of vibrational properties of PSII, for example, in the spectral range related to the vibrational modes of the carbonyl groups of chlorophyll-*a*.

In the present work, we have chosen to study the IR spectrum of the chlorophyll-*a* cation, modeled by chlorophyll-*a5*, with 64 atoms and 186 normal modes, in the gas phase and in tetrahydrofuran (THF) solution. The computations have been performed at the B3LYP/N07D level and the effect of the tetrahydrofuran solvent has been included by means of the conductor-like polarizable continuum model [73]. From the overall IR spectrum of chlorophyll-*a*, the spectral region around 1700 $cm^{-1}$ (see Fig. 3) shows specific features, so we have chosen to compute anharmonic frequencies only for the three modes related to the most distinct C=O bands, as reported in Table V. The assignment proposed in Ref. 91 has been adopted in this work, and confirmed by visual inspection of the nuclear displacements. The reduced dimensionality VPT2 computations allowed for a quantitatively reliable comparison between calculated and experimental spectra, including anharmonic and environmental effects.

Considering that the spectrum energy range considered is solely related to the vibrations of the carbonyl group, couplings to other modes are expected to be rather small. The reliability of the results is then checked analyzing the most pronounced coupling terms as suggested before. It is observed that coupling terms are generally small, and the most pronounced ones are related to the coupling of modes 26 and 27 with mode 25, so within the set of the normal coordinates considered in the force constants evaluation. In fact, in the gas phase, all coupling terms are negligible, as confirmed by agreement within 2 $cm^{-1}$ between one-mode and three-mode computations. Solvent effects lead to an increase of $K_{iij}$ related to the coupling between modes 27 and 25, which is however included if all three modes are computed together. Additionally, analysis of $\sum |K_{iij}|$ and $|K_{iij}|_{\max}$ shows that all non-negligible effects have been taken into account.

Figure 3 compares the spectra computed within and beyond the harmonic approximation, in the gas phase and in tetrahydrofuran solution to the experimental FTIR absorbance spectra of chlorophyll-a in deuterated tetrahydrofuran after cation formation [92]. It is shown that the best agreement with experimental results is obtained when both solvent and anharmonic effects are taken into account simultaneously, while each of the effects taken into account separately leads to the improvement over the harmonic computations in the gas phase. It is remarkable to be noted that anharmonic frequencies for chlorophyll-a in THF solution, computed with reduced-dimensional VPT2 treatment match almost exactly the experimental data. This result shows clearly that the reduced-dimensionality aharmonic computations pave a feasible route to improve

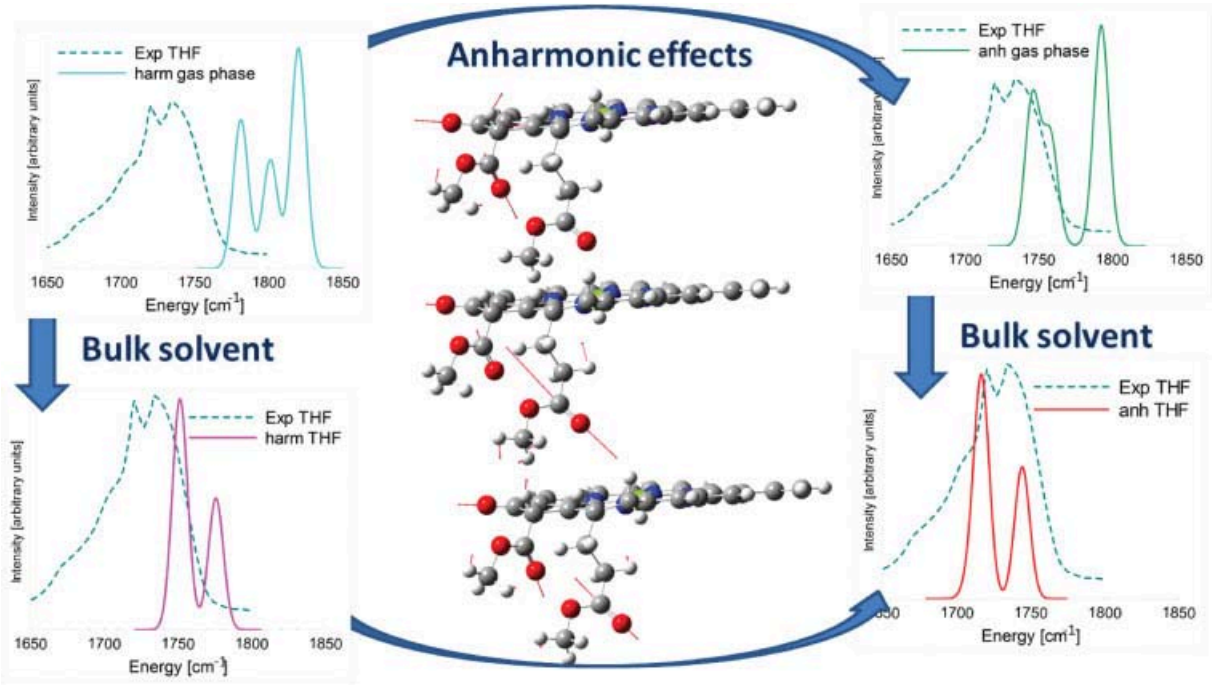


**FIGURE 3.** Vibrational harmonic and anharmonic spectra of the chlorophyll-*a* cation in the gas phase and in tetrahydrofuran solution. [Color figure can be viewed in the online issue, which is available at wileyonlinelibrary.com.]

accuracy of computed spectra for significantly large systems of biological interest.

## 5. Conclusions

The reduced-dimensionality VPT2 treatment has been discussed and formalized. It has been demonstrated that such an approach allows for the direct evaluation of some experimentally observable frequencies and can be successfully applied to rather large systems, providing a viable route to improve the understanding of observed experimentally frequency shifts related to environmental effects, adsorption on a surface or macromolecular embedding. For such extended systems, it is possible to study anharmonic effects for some selected modes of interest only, for example, corresponding to the

**TABLE V**

**Anharmonic vibrational frequencies of Chlorophyll-*a* cation in gas phase and tetrahydrofuran solution computed considering each mode one-by-one (1M) or taking into account all couplings between C=O vibrations (3M). Sum of nondiagonal cubic force constants, $\sum |K_{ij}|$ with respect to *i*th normal mode and the value of the largest anharmonic contribution to the *i*th normal mode $|K_{ij}|_{max}$, and the corresponding $j_{max}$ index are also reported.**

| Mode | Assignment[a] | 1M | 3M | $\sum \lvert K_{ij} \rvert$ | $\lvert K_{ij} \rvert_{max}$ | $j_{max}$ |
|---|---|---|---|---|---|---|
| | | | Vacuum | | | |
| 25 | $\nu(13^1$ and $13^3$ C=O)*s* | 1792 | 1790 | 3 | −1 | 2 |
| 26 | $\nu(17^3$ − ester C=O) | 1741 | 1742 | 25 | 10 | 25 |
| 27 | $\nu(13^1$ and $13^3$ C=O)*as* | 1743 | 1744 | 110 | 80 | 25 |
| | | | Tetrahydrofuran | | | |
| 25 | $\nu(13^1$ and $13^3$ C=O)*s* | 1750 | 1747 | 3 | 1 | 19 |
| 26 | $\nu(17^3$ − ester C=O) | 1712 | 1713 | 27 | 15 | 25 |
| 27 | $\nu(13^1$ and $13^3$ C=O)*as* | 1706 | 1720 | 369 | 347 | 25 |

[a]Assignment from the Ref. [91].

most intense bands in the IR spectrum, a selected spectral range or the molecular probe. Two examples, namely glycine adsorbed on a silicon cluster and chlorophyll-*a* in solution, highlight the feasibility and accuracy of presented anharmonic approach. For glycine adsorbed on a silicon surface computations taking into account only the high-frequency modes of glycine are compared with study where all the normal modes of glycine molecule have been considered. For chlorophyll-*a* only, the modes related to the C=O stretchings have been taken into account, but it was sufficient to significantly improve the agreement with experimental results, the accuracy being further enhanced by simulating environmental effects with the continuum solvent model. The cases discussed in the present work suggest a practical path for reduced dimensionality VPT2 computations: the sets of normal modes to be considered simultaneously are selected based on the nature of the vibrations and the related energy range. In this way, all vibrations mainly localized on the same region of a molecular system (e.g., functional group) and with similar frequencies, which are likely to be coupled, are included in the anharmonic treatment. Results from this work show that such properly tailored reduced-dimensionality anharmonic approaches pave a feasible route toward the state-of-the-art computational spectroscopy studies and allow to take into account simultaneously anharmonic and environmental effects on the vibrational spectra even for relatively large molecular systems.

### ACKNOWLEDGMENTS

The large scale computer facilities of the VILLAGE network (http://m3village.sns.it) and the Wroclaw Centre for Networking and Supercomputing are acknowledged for providing computer resources.

## References

1. Jensen, P.; Bunker, P. R., Eds. Computational Molecular Spectroscopy; Wiley: UK, 2000.
2. Matyus, E.; Czako, G.; Csaszar, A. J Chem Phys 2009, 130, 134112.
3. Cappelli, C.; Biczysko, M. In Computational Strategies for Spectroscopy, from Small Molecules to Nano Systems; Barone, V., Ed.; Wiley: Hoboken, NJ, 2011.
4. Pedone, A.; Biczysko, M.; Barone, V. Comput Phys Commun 2010, 11, 1812.
5. Vreven, T.; Morokuma, K. J Comput Chem 2000, 21, 1419.
6. Vreven, T.; Morokuma, K.; Farkas, O.; Schlegel, H. B.; Frisch, M. J. J Comput Chem 2003, 24, 760.
7. Rega, N.; Iyengar, S. S.; Voth, G. A.; Schlegel, H. B.; Vreven, T.; Frisch, M. J. J Phys Chem B 2004, 108, 4210.
8. Barone, V.; Biczysko, M.; Brancato, G. Adv Quantum Chem 2010, 59, 17.
9. Cappelli, C.; Monti, S.; Scalmani, G.; Barone, V. J Chem Theory Comput 2010, 6, 1660.
10. Begue, D.; Carbonniere, P.; Barone, V.; Pouchan, C. Chem Phys Lett 2005, 416, 206.
11. Hirata, S.; Yagi, K. Chem Phys Lett 2008, 464, 123.
12. Braams, B. J.; Bowman, J. M. Int Rev Phys Chem 2009, 28, 577.
13. Sparta, M.; Høyvik, I.; Toffoli, D.; Christiansen, O. J Phys Chem A 2009, 113, 8712.
14. Pele, L.; Gerber, R. J Chem Phys 2008, 128, 165105.
15. Carter, S.; Handy, C. Chem Phys Lett 2002, 352, 1.
16. Bowman, J. M. Science 2000, 290, 724.
17. Bowman, J. M.; Carter, S.; Huang, X. Int Rev Phys Chem 2003, 22, 533.
18. Carter, S.; Handy, N. J Chem Phys 2000, 113, 987.
19. Chaban, J.; Jung, J.; Gerber, R. J Chem Phys 1999, 111, 1823.
20. Yagi, K.; Taketsugu, T.; Hirao, K.; Gordon, M. S. J Chem Phys 2000, 113, 1005.
21. Rauhut, G.; Pulay, P. J Phys Chem 1995, 99, 3093.
22. Rauhut, G.; Hrenar, T. Chem Phys 2008, 346, 160.
23. Christiansen, O. Phys Chem Chem Phys 2007, 9, 2942.
24. Norris, L. S.; Ratner, M. A.; Roitberg, A. E.; Gerber, R. B. J Chem Phys 1996, 105, 11261.
25. Christiansen, O. J Chem Phys 2003, 119, 5773.
26. Carter, S.; Sharma, A. R.; Bowman, J. M.; Rosmus, P.; Tarroni, R. J Chem Phys 2009, 131, 224106.
27. Christiansen, O. J Chem Phys 2004, 120, 2149.
28. Pouchan, C.; Zaki, K. J Chem Phys 1997, 107, 342.
29. Carbonniere, P.; Dargelos, A.; Pouchan, C. Theor Chim Acta 2010, 125, 543.
30. Mills, I. M. Molecular Spectroscopy: Modern Research; Academic: press: New York, 1972.
31. Amos, R. D.; Handy, N. C.; Green, W. H.; Jayatilaka, D.; Willets, A.; Palmieri, P. J Chem Phys 1991, 95, 8323.
32. Gaw, F.; Willetts, A.; Handy, N. C.; Green, W. In Advances in Molecular Vibrations and Collision Dynamics; JAI Press: Greenwich, CT, 1990.
33. Barone, V. J Chem Phys 2005, 122, 014108.
34. Barone, V. J Chem Phys 2004, 120, 3059.
35. Martin, J. M. L.; Lee, T. J.; Taylor, P. R.; Francois, J.-P. J Chem Phys 1995, 103, 2589.
36. Stanton, J. F.; Gauss, J. J Chem Phys 1998, 108, 9218.
37. Tew, D. P.; Klopper, W.; Heckert, M.; Gauss, J. J Phys Chem A 2007, 111, 11242.
38. Ruud, K.; Taylor, P. R.; Helgaker, T. J Chem Phys 2003, 119, 1951.
39. Ruud, K.; Åstrand, P. O.; Taylor, P. R. J Chem Phys 2000, 112, 2668.
40. Vazquez, J.; Stanton, J. F. Mol Phys 2006, 104, 377.
41. Vazquez, J.; Stanton, J. F. Mol Phys 2007, 105, 101.

42. Stanton, J. F.; Gauss, J. Int Rev Phys Chem 2000, 19, 61.
43. Bloino, J.; Guido, C.; Lipparini, F.; Barone, V. Chem Phys Lett 2010, 496, 157.
44. Miani, E.; Can, E.; Palmieri, P.; Trombetti, A.; Handy, N. C. J Chem Phys 2000, 112, 248.
45. Burcl, R.; Handy, N. C.; Carter, S. Spectrochim Acta A 2003, 59, 1881.
46. Boese, A. D.; Martin, J. J Phys Chem A 2004, 108, 3085.
47. Barone, V. J Phys Chem A 2004, 108, 4146.
48. Barone, V.; Festa, G.; Grandi, A.; Rega, N.; Sanna, N. Chem Phys Lett 2004, 388, 279.
49. Biczysko, M.; Panek, P.; Barone, V. Chem Phys Lett 2009, 475, 105.
50. Bloino, J.; Biczysko, M.; Crescenzi, O.; Barone, V. J Chem Phys 2008, 128, 244105.
51. Becke, A. D. J Chem Phys 1993, 98, 5648.
52. Carbonniere, P.; Lucca, T.; Pouchan, C.; Rega, N.; Barone, V. J Comput Chem 2005, 26, 384.
53. Boese, A. D.; Martin, J. J Phys Chem A 2004, 108, 3085.
54. Barone, V. Chem Phys Lett 2004, 383, 528.
55. Barone, V.; Grandi, A.; Rega, N.; Sanna, N. Chem Phys Lett 2004, 388, 279.
56. Barone, V.; Bloino, J.; Biczysko, M. Phys Chem Chem Phys 2010, 12, 1092.
57. Puzzarini, C.; Biczysko, M.; Barone, V. J Chem Theory Comput 2010, 6, 828.
58. Grimme, S. J Chem Phys 2006, 124, 034108/1–16.
59. Neese, F.; Schwabe, T.; Grimme, S. J Chem Phys 2007, 126, 124115.
60. Biczysko, M.; Panek, P.; Scalmani, G.; Bloino, J.; Barone, V. J Chem Theory Comput 2010, 6, 2115.
61. Kozuch, S.; Gruzman, D.; Martin, J. M. L. J Phys Chem C 2010, 114, 20801.
62. Begue, D.; Carbonniere, P.; Pouchan, C. J Phys Chem A 2005, 109, 4611.
63. Begue, D.; Benidar, A.; Pouchan, C. Chem Phys Lett 2006, 430, 215.
64. Puzzarini, C.; Barone, V. J Chem Phys 2008, 129, 084306/1–7.
65. Puzzarini, C.; Barone, V. Phys Chem Chem Phys 2008, 10, 6991.
66. Kuhler, K. M.; Truhlar, D. G.; Isaacson, A. D. J Chem Phys 1996, 104, 4664.
67. Miller, W. H.; Hernandez, R.; Handy, N. C.; Jayatilaka, D.; Willets, A. Chem Phys Lett 1990, 172, 62.
68. Barone, V.; Cimino, P.; Stendardo, E. J Chem Theory Comput 2008, 4, 751.
69. Barone, V.; Cimino, P. Chem Phys Lett 2008, 454, 139.
70. Barone, V.; Cimino, P. J Chem Theory Comput 2009, 5, 192.
71. Double and triple-$\zeta$ basis sets of N07 family, are available for download, visit http://idea.sns.it (accessed April 20, 2011).
72. Barone, V.; Biczysko, M.; Cimino, P. In Carbon-Centered Free Radicals and Radical Cations; Forbes, M. D. E., Ed.; Willey: Hoboken, NJ, 2010; pp 105–139.
73. Cossi, M.; Scalmani, G.; Rega, N.; Barone, V. J Comput Chem 2003, 24, 669.
74. Frisch, M. J.; Trucks, G. W.; Schlegel, H. B.; Scuseria, G. E.; Robb, M. A.; Cheeseman, J. R.; Montgomery, J. A., Jr.; Vreven, T.; Kudin, K. N.; Burant, J. C.; Millam, J. M.; Iyengar, S. S.; Tomasi, J.; Barone, V.; Mennucci, B.; Cossi, M.; Scalmani, G.; Rega, N.; Petersson, G. A.; Nakatsuji, H.; Hada, M.; Ehara, M.; Toyota, K.; Fukuda, R.; Hasegawa, J.; Ishida, M.; Nakajima, T.; Honda, Y.; Kitao, O.; Nakai, H.; Klene, M.; Li, X.; Knox, J. E.; Hratchian, H. P.; Cross, J. B.; Bakken, V.; Adamo, C.; Jaramillo, J.; Gomperts, R.; Stratmann, R. E.; Yazyev, O.; Austin, A. J.; Cammi, R.; Pomelli, C.; Ochterski, J. W.; Ayala, P. Y.; Morokuma, K.; Voth, G. A.; Salvador, P.; Dannenberg, J. J.; Zakrzewski, V. G.; Dapprich, S.; Daniels, A. D.; Strain, M. C.; Farkas, O.; Malick, D. K.; Rabuck, A. D.; Raghavachari, K.; Foresman, J. B.; Ortiz, J. V.; Cui, Q.; Baboul, A. G.; Clifford, S.; Cioslowski, J.; Stefanov, B. B.; Liu, G.; Liashenko, A.; Piskorz, P.; Komaromi, I.; Martin, R. L.; Fox, D. J.; Keith, T.; Al-Laham, M. A.; Peng, C. Y.; Nanayakkara, A.; Challacombe, M.; Gill, P. M. W.; Johnson, B.; Chen, W.; Wong, M. W.; Gonzalez, C.; Pople, J. A. Gaussian 09, Revision B.01; Gaussian, Inc.: Wallingford, CT, 2009.
75. Hoffmann, L. J. H.; Marquardt, S.; Gemechu, A. S.; Baumgärtel, H. Phys Chem Chem Phys 2006, 8, 2360.
76. Balfour, W. J. Spectrochim Acta Part A 1983, 39, 795.
77. Chaban, G.; Jung, J.; Gerber, R. J Phys Chem A 2000, 104, 10035.
78. Bludsky, O.; Chocholousova, J.; Vacek, J.; Huisken, F.; P., H. J Chem Phys 2000, 113, 11.
79. Espinoza, C.; Szczepanski, J.; Vala, M.; Polfer, N. J Phys Chem A 2010, 114, 5919.
80. Carnimeo, I; Biczysko, M.; Bloino, J.; Barone, V. Phys Chem Chem Phys 2011, 13. In press.
81. Huisken, F.; Werhahn, O.; Ivanov, A.; Krasnokutski, S. J Chem Phys 1999, 111, 7.
82. Stepanian, S.; Reva, I.; Radchenko, E.; Rosado, M.; Duarte, M.; Fausto, R.; Adamowicz, L. J Phys Chem A 1998, 102, 1041.
83. Espinoza, C.; Szczepanski, J.; Vala, M.; Polfer, N. J Phys Chem A 2010, 114, 5919.
84. Shemesh, D.; Mullin, J.; Gordon, M.; Gerber, R. Chem Phys 2008, 347, 218.
85. Lopez, A.; Heller, T.; Bitzer, T.; Richardson, N. Chem Phys 2002, 277, 1.
86. Vassiliev, S.; Bruce, D. Photosynth Res 2008, 97, 75.
87. Loll, B.; Kern, J.; Saenger, W.; Zouni, A.; Biesiadka, J. Nature 2005, 438, 1040.
88. Nelson, N.; Yocum, C. F. Annu Rev Plant Biol 2006, 57, 521.
89. Muller, M. G.; Slavov, C.; Luthra, R.; Redding, K. E.; Holzwarthet, A. R. Proc Natl Acad Sci 2010, 107, 4123.
90. Wang, R.; Parameswaran, S.; Hastings, G. Vib Spectrosc 2007, 44, 357.
91. Parameswaran, S.; Wang, R.; Hastings, G. J Phys Chem B 2008, 112, 14056.
92. Nabedryk, E.; Leonhard M., W., Mantele; Breton, J. Biochemistry 1990, 29, 3242.